

# Bending-Beam Measurement of Solvent Diffusions in Polyimides: Theoretical and Experimental

JWO-HUEI JOU\* and LI HSU

Department of Materials Science and Engineering, Tsing Hua University, Hsin Chu 30043, Taiwan, R. O. C.

## SYNOPSIS

A general formula correlating the bending curvature variation ratio of a layered structure caused by solvent-induced swelling in its polymer overcoat with diffusion time under case II diffusion has been presented. In the event of case II diffusion, the diffusion front velocity,  $v$ , can be calculated by using this formula and measured by a bending-beam apparatus. At room temperature, the diffusion of *n*-methyl-pyrrolidone (NMP) solvent in the film of pyromellitic phenylene diamine (PMDA-PDA) is case II. While in PMDA-B (-benzidine) and benzophenone tetracarboxylic dianhydride (BPDA-PDA), no diffusion progress can be observed. But, the diffusion in 6F-dianhydride- (6FDA-PDA) is case I with  $D = 0.85 \times 10^{-9} \text{ cm}^2/\text{s}$ . It becomes anomalous when mixing with 25% PMDA-B, but becomes case II diffusion with more PMDA-B. The preabsorbed moisture in the films does not affect the  $v$  value. In PMDA-PDA,  $v = 7.3 \times 10^{-8} \text{ cm/s}$ . In the 25/75 and 50/50 6FDA-PDA/PMDA-B blends,  $v = 6.3$  and  $11.3 \times 10^{-8} \text{ cm/s}$ .

## INTRODUCTION

Polyimide films exhibit excellent mechanical properties, low dielectric constant, high glass transition temperature, and low thermal expansion coefficient.<sup>1,2</sup> They can be used as interlayer dielectrics,  $\alpha$ -particle protection coating, and thermal-mechanical buffer layers in microelectronic devices.<sup>3-7</sup> During the fabrication of these devices, the polyimide films may be spin-cast a layer of photoresist. After certain processes, the photoresist layer will be removed from the polyimide films. This is usually done by using stripping agents, such as *n*-methylpyrrolidone (NMP) solvent. The polyimide films will then be exposed to the solvent and swell. This swelling behavior may have some undesired impacts. Furthermore, in the fabrication for multilevel interconnection packaging the polyimide films would be in a multilayered form. The preformed layers of polyimide will be exposed to the solvent from the later cast films of polyamic acids, for example. In this case, diffusion of solvent into the preformed

films will also result in swelling, enabling the diffusion of polyamic acids into the solid polyimides. Such a diffusion behavior is crucial to the strength of autoadhesion of the two neighboring layers.<sup>8</sup> Therefore, it is definitely necessary to have a thorough understanding of the characteristics of solvent diffusion in polyimide films.

Diffusions of solvents in polyimide films have been studied for a few years.<sup>9-11</sup> In these studies, only the semi-flexible polyimide pyromellitic dianhydride-4,4'-oxydianiline PMDA-ODA has been most intensively examined. Other semiflexible or rigid rod-like polyimides have not been much studied. Therefore, it is our intention to investigate the diffusions of solvent in several different polyimides with semiflexible and rigid rod-like chain structures. The polyimides chosen for this study are semiflexible 6F-dianhydride-*p*-phenylenediamine (6FDA-PDA), rigid rod-like pyromellitic phenylene diamine (PMDA-PDA), pyromellitic-benzidine (PMDA-B), and 3,3',4,4'-benzophenone tetracarboxylic dianhydride-phenylene diamine (BPDA-PDA), and their blends.

Many techniques have been used to study the transport of solvents in polymers. They include techniques of using a piezoelectric quartz microbal-

\* To whom correspondence should be addressed.

ance, digibridge capacitor, interferometer, bending-beam apparatus, and Rutherford backscattering spectrometer, etc.<sup>10-15</sup> Among these, the bending beam technique is a relatively convenient and sensitive method. It has been successfully applied by Berry et al.<sup>14</sup> and Jou et al.<sup>16,17</sup> in the measurements of the diffusions of moisture or water in epoxy coatings on copper sheets and polyimide films on silicon substrates, respectively. These diffusions all belong to case I. Due to mathematical complications, no theoretical model has yet been developed for the bending-beam diffusion technique in the event of case II diffusion. This will, consequently, greatly limit the usage of the technique because many solvent diffusions in polymer films are case II diffusion. In this report, we will present a new developed model for the bending-beam diffusion technique for case II diffusion. According to the model, we are able to determine the diffusion front velocity constants of NMP solvent diffusion in various polyimide films using a modified bending-beam apparatus.

## THEORY

The diffusion of solvents in various polymers has been found to obey a case II diffusion mechanism.<sup>18</sup> Case II diffusion can be characterized as follows: (1) upon sorption, the weight gain with respect to time is linear; (2) a sharp swelling interface separates the inner unswollen region from the outer swollen region, and there is a uniform concentration of penetrant across the swollen layer; and (3) the sharp swelling interface advances at a constant velocity. As known, a given polymer will swell upon uptaking solvent during diffusion. If the polymer is cast as a film on a layered substrate, swelling in the polymer film will cause the substrate to bend. By measuring the change of the bending curvature in the polymer-coated bilayered structure, one would be able to monitor the diffusion process if the bending curvature variation of the structure, caused by solvent diffusion-induced swelling in its polymer overcoat, can be correlated to diffusion time. Such a correlation has been established according to the characteristics mentioned above and will be described in the following section.

At any diffusion time,  $t$ , the polymer overcoat can be divided into two layers, one of which is for the unswollen region and the other the swollen region. As shown in the schematic diagram of Figure 1, the unswollen and swollen layers are denoted as 2 and 3 and with thicknesses of  $d_2(t)$  and  $d_3(t)$ , respectively. The difference between the swollen and

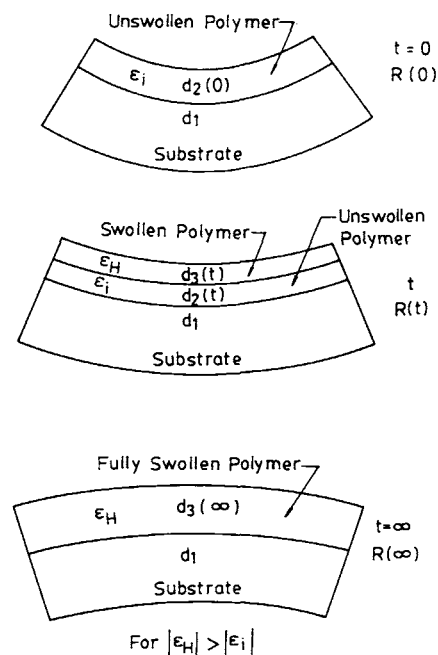


**Figure 1** Schematic diagram of a layered substrate coated with a polymer film upon solvent diffusion. The film is divided into swollen and unswollen parts with layer thicknesses of  $d_3(t)$  and  $d_2(t)$ , respectively, at a given diffusion time,  $t$ .

unswollen layers is that there is a hygroscopic strain in the swollen layer while both layers may, in most cases, have an intrinsic strain upon casting and curing prior to diffusion. Since layers 2 and 3 in Figure 1 have different mechanical characteristics, including the substrate layer 1, the whole structure should be treated as a trilayer structure. Similar to the method used in deriving other models,<sup>19-22</sup> we derive this model according to the three general balance equations. These equations consist of an internal force balance, internal strain change balances at interfaces, and a moment balance.

### Internal Force Balance

According to the force balance equation, summation of the internal forces in the three different layers should be equal to zero at any given diffusion time,  $t$ .

$$F_1(t) + F_2(t) + F_3(t) = 0. \quad (1)$$

### Strain Change Balance at Interface

At interfaces, upon diffusion, the variations of the internal strains of any two neighboring layers should be equal and one has the following relations.

$$\frac{F_1(t)}{Wd_1E_1^*} - \frac{d_1}{2R(t)} = \epsilon_i + \frac{F_2(t)}{Wd_2(t)E_2^*} + \frac{d_2(t)}{2R(t)} \quad (2)$$

$$\begin{aligned} \epsilon_i + \frac{F_2(t)}{Wd_2E_2^*} - \frac{d_2(t)}{2R(t)} \\ = \epsilon_i + \frac{F_3(t)}{Wd_3(t)E_3^*} + \frac{d_3(t)}{2R(t)} + \epsilon_H, \quad (3) \end{aligned}$$

where  $E^*(t)$  is denoted as biaxial modulus,  $E(t)/(1 - \nu)$ , and  $E$  and  $\nu$  Young's modulus and Poisson's ratio. Width is denoted as  $W$ .  $R$  is the bending curvature radius of the trilayer structure.  $\epsilon_i$  is denoted as the intrinsic strain in the 2 and 3 layers and  $\epsilon_H$  the hygroscopic strain in the swollen 3 layer of Figure 1.

The hygroscopic strain  $\epsilon_H$  is defined as

$$\epsilon_H = SC_o. \quad (4)$$

where  $C_o$  is the concentration of penetrant or solvent in the swollen layer and  $S$  is the linear swelling parameter of the polymer film. The polymer film may be elastically anisotropic; i.e., its mechanical properties in the film plane direction may be different from those in the transverse direction. Consequently, the linear swelling parameters in the plane and transverse directions may not be the same. However, in layered structures, only those properties in the plane directions are considered. The linear swelling parameter,  $S$ , used here is for the plane direction and will not be specified in later derivation.

### Moment Balance

In this balance equation, the total moment of the internal forces should be counteracted by that due to bending. Therefore, one obtains

$$\begin{aligned} M_1(t) + M_2(t) + M_3(t) \\ + F_1(t)\left(\frac{d_1}{2}\right) + F_2(t)\left(d_1 + \frac{d_2(t)}{2}\right) \\ + F_3(t)\left(d_1 + d_2(t) + \frac{d_3(t)}{2}\right) = 0, \quad (5) \end{aligned}$$

where

$$M_i(t) = \frac{WE_i^*d_i^3(t)}{12R(t)}, \quad i = 1, 2, 3.$$

From eqs. (1), (2), (3), and (5), the radius of bending curvature,  $R(t)$ , can be expressed in the terms of the mechanical and time-dependent and

time-independent geometric parameters. It is, of course, also a function of the intrinsic and hygroscopic strains. Without simplification, the expression for  $R(t)$  will be very lengthy and complex. However, in most cases, it is usually true that  $d_2$  or  $d_3 \ll d_1$  and  $E_2$  or  $E_3 < E_1$ . One can therefore express the bending curvature radius,  $R(t)$ , in a much simplified way as follow.

$$1/R(t) = \frac{6E_1^*d_1^2(E_2^*d_2(t) + E_3^*d_3(t))\epsilon_i + 6E_1^*d_1^2E_3^*d_3(t)\epsilon_H}{(E_1^*)^2(d_1)^4}. \quad (6)$$

According to this equation, the initial bending curvature  $1/R(0)$  can be expressed as

$$1/R(0) = \frac{6E_1^*d_1^2E_2^*d_2(0)\epsilon_i}{(E_1^*)^2(d_1)^4}, \quad (7)$$

where  $d_2(0)$  is the initial film thickness before diffusion takes place. The bending curvature at equilibrium,  $1/R(\infty)$ , can be expressed as

$$1/R(\infty) = \frac{6E_1^*d_1^2E_3^*d_3(\infty)(\epsilon_i + \epsilon_H)}{(E_1^*)^2(d_1)^4}, \quad (8)$$

where  $d_3(\infty)$  is the final thickness of the fully swollen polymer film at equilibrium.

As mentioned earlier, in case II diffusion there will be a sharp diffusion front. The diffusion front will advance at a constant velocity. This diffusion front velocity,  $v$ , is the most important parameter to be determined. Therefore, an expression correlating the diffusion front velocity with the bending curvature should be derived. This can be obtained as follows.

In the diffusion process, if

$$d_2(0)E_2^*(0) = Cd_3(\infty)E_3^*(\infty), \quad (9)$$

a very useful and simple relation for the bending curvature variation ratio with the diffusion front velocity can be reached. In the above equation,  $C$  is an arbitrary constant.  $C$  should be equal to or greater than 1. If the uptaken solvent does not affect the intermolecular interaction of the polymer chains, the polymer film would just swell and its apparent biaxial modulus,  $E_3^*$ , would decrease and be in proportion to the ratio of  $d_2(0)/d_3(\infty)$ . In such a case,  $C = 1$ . It is noteworthy that  $d_2(0)$  is always smaller than  $d_3(\infty)$ . If the absorbed solvent would plasticize the polymer or weaken its intermolecular force, the apparent biaxial modulus of the swollen film,  $E_3^*$ ,

would decrease even more and would be proportional to a ratio of  $Cd_2(0)/d_3(\infty)$ . In this case,  $C > 1$ .

However, whether  $C = 1$ ,  $> 1$ , or  $< 1$  (which is very unlikely to happen), based on eq. (9) one can obtain the following formula.

$$\Omega = \frac{1/R(t) - 1/R(0)}{1/R(\infty) - 1/R(0)} = \frac{d_3(t)}{d_3(\infty)}, \quad (10)$$

where  $\Omega$  is a dimensionless bending curvature variation ratio as defined above.

Once the polymer film is swelling,  $d_3(t) = S_T vt$ .  $S_T$  is the linear swelling parameter of the polymer film in the transverse direction, and is defined as  $S_T = d_3(\infty)/d_2(0)$ . One therefore has  $d_3(t) = vt d_3(\infty)/d_2(0)$ . By substituting this term back into eq. (10), the formula that correlates the bending curvature variation ratio with the diffusion time can be resulted.

$$\Omega = \frac{vt}{d_2(0)}. \quad (11)$$

As seen, by measuring the bending curvature variation ratio,  $\Omega$ , with time, and by knowing the initial film thickness, one can readily obtain the diffusion front velocity,  $v$ .

## EXPERIMENTAL

### Materials

The starting materials used in this study are dianhydrides—PMDA, BPDA, and 6FDA—and diamines—*p*-phenylenediamine (PDA) and benzidine (B). The solvent is *N*-methyl pyrrolidone (NMP). These materials were used as received.

### Polycondensation of Polyamic Acids

PMDA-PDA, BPDA-PDA, 6FDA-PDA, and PMDA-B polyamic acids were prepared as follows<sup>23</sup>: In a four-neck round bottle flask, diamine (PDA or B) was dissolved in the NMP solvent. When the diamine had been completely dissolved, equal molar dianhydride (PMDA, BPDA, or 6FDA) was added gradually. The reaction proceeded for 5 h with stirring. The entire process was done under nitrogen atmosphere. The resulting solution had a solid content of 14 wt %. The molecular structures of the resulted polyamic acids (after cured to solid imides) are shown in Figure 2.

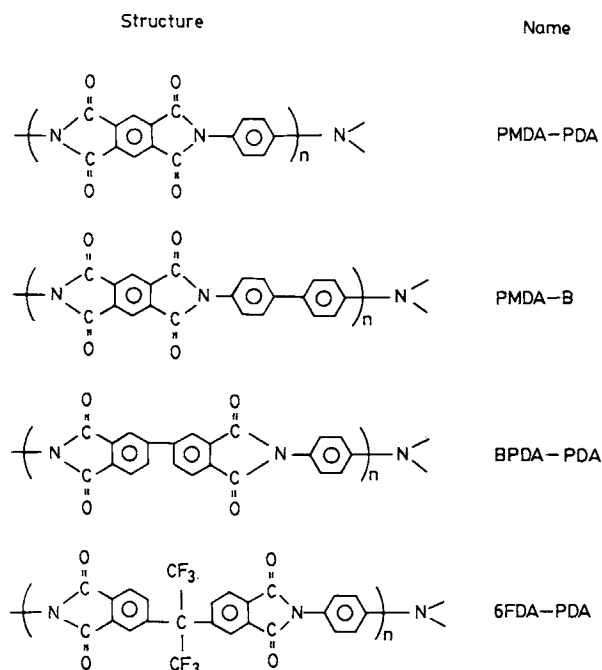


**Figure 2** Molecular structures of the studied polyimides.

### Polyimide Blend

Blend of 6FDA-PDA with PMDA-B was obtained by mixing the resulted polyamic acids. The mixing was done under nitrogen atmosphere for 20 min. The resulting mixed solutions were heated at 50°C for 40 h, and then cooled and kept frozen before use.

### Imidization

Solid films of the above-mentioned polyamic acids were prepared by spin-casting the solutions on glass substrates. This was followed by prebaking at 80°C for 30 min, and then curing from 80 to 350°C in 3 h. These films were used for X-ray diffraction experiments.

### Bending-Beam Specimen Preparation

The substrates used for bending curvature measurement are silicon strips with 7.5 cm in length, 0.5 cm in width, and 390  $\mu\text{m}$  in thickness. These silicon strips were prepared by slicing (100) silicon wafers along the (100) crystal plane. Polyimide films were prepared by spin-casting their polyamic acid solutions on the substrates, followed by prebaking at 80°C for 30 min, and then cured to 350°C. Since one end of the substrate must be mounted on a clamp and the other end must reflect laser beam to a sensor, the two ends of the solid film were removed by 1 cm.

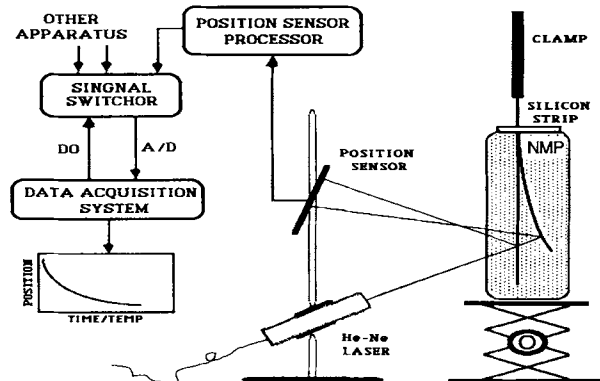


**Figure 3** Schematic illustration of the experiment setup of the bending-beam apparatus used for the solvent diffusion measurements.

### Bending Curvature Measurement

Figure 3 shows a schematic diagram of the experiment setup for bending curvature measurement. Before being measured, the samples were kept in a vacuum chamber to prevent moisture uptake. To study the moisture effect on solvent diffusion, samples were kept in air with 55% humidity for several days before measurement. To measure its bending curvature by using the bending-beam apparatus, the specimen was mounted on a clamp. The deflection of the free end of the specimen was measured continuously during solvent diffusion. According to the geometry of the setup, the obtained deflection position data was then converted to bending curvature,  $1/R$ .

### X-Ray Specimen Preparation and Experiment

For the X-ray experiment, polyimide films of about 15 to 20  $\mu\text{m}$  thick were prepared. In a previous X-ray experiment, it was found that these polyimide films must be thicker than 200  $\mu\text{m}$  so that the X-ray will not penetrate through the films. To compare quantitatively, relatively thick samples are therefore required. This was done by stacking many pieces, around fifty or so, of the films together. In this study, out-of-plane diffraction patterns of the resulting specimens are presented. Each resulting diffraction pattern provides information concerning the intermolecular ordering of its corresponding imide chain and can be used to characterize the morphology of its corresponding polyimide film.<sup>24</sup>

X-ray experiments were done using a Rigaku wide-angle X-ray diffractometer with a nickel-filtered copper  $K\alpha_1$ -radiation. Its power setting was at 40 kV and 20 mA. The line-focus slot has a di-

mension of  $8 \times 0.04$  mm. Details regarding X-ray specimen preparation and experiment can be found in the paper by Jou and Huang.<sup>24</sup>

## RESULTS AND DISCUSSION

### Case II Diffusion and Moisture Effect

The diffusion of NMP solvent in the imide film of PMDA-PDA at room temperature is shown in Figure 4. As seen, the dimensionless bending curvature variation ratio vs. diffusion time is linear after a short period of time. Except in the very beginning, these experimental data demonstrate that the diffusion of NMP in the film is a case II diffusion. From the slope of the linear part of the curve, one can calculate the diffusion front velocity according to eq. (11). The calculated diffusion front velocity,  $v$ , is  $7.3 \times 10^{-8}$  cm/s for the PMDA-PDA imide film with a thickness of 12.3  $\mu\text{m}$ .

Figure 5 shows the effect of the presence of the preabsorbed moisture in the film on the experimental diffusion curve. As known, water and NMP are miscible to each other. The absorbed water would desorb when the film is immersed into the NMP solvent. If the desorption of water is much faster than the sorption of NMP, in the beginning the specimen will bend to a direction opposite to that caused by solvent-absorption-induced swelling because desorption of water will cause shrinkage in the film. This phenomenon can be seen in the plot for  $t/d_2(0) < 0.22 \times 10^7$  s/cm. At a certain time,

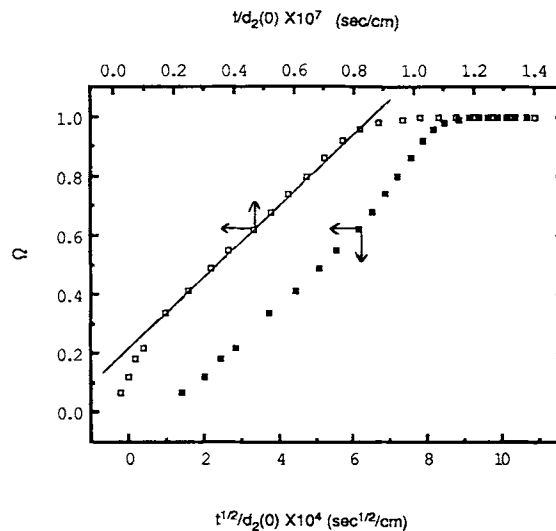


**Figure 4** The measured bending curvature variation ratio vs. diffusion time of the diffusion of NMP solvent in the imide film of PMDA-PDA at room temperature.

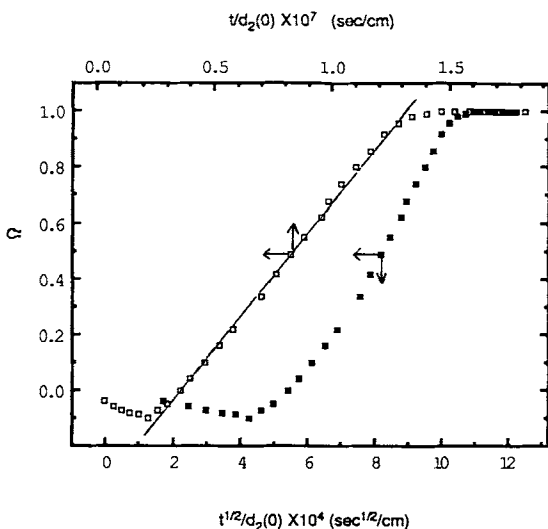


**Figure 5** The measured bending curvature variation ratio vs. diffusion time of the diffusion of NMP solvent in the imide film of PMDA-PDA under the effect of preabsorbed moisture at room temperature.

the effect of water-desorption-induced shrinkage will be counteracted by that of NMP-absorption-induced swelling. In such a case, the specimen will stop bending at that specific moment; it is  $t/d_2(0) = 0.22 \times 10^7$  s/cm in this case. For  $t/d_2(0) > 0.22 \times 10^7$  s/cm, water-desorption-induced shrinkage becomes less and less important and NMP-absorption-induced swelling becomes dominant. This results in the change of bending direction. From Figure 5, one can calculate the diffusion coefficient of water desorption as well as the diffusion front velocity. The water desorption diffusion coefficient as calculated is  $0.52 \times 10^{-9}$  cm<sup>2</sup>/s, and  $v$  is  $7.1 \times 10^{-8}$  cm/s. The diffusion coefficient was computed using a model presented in a separate paper.<sup>16</sup> It can be also calculated using the model by Berry.<sup>14</sup> However, using the latter model for the diffusion coefficient calculation requires a complicated numerical computation. The diffusion coefficients of water absorption in the imide films of PMDA-PDA immersed in water and exposed in air are  $1.25$  and  $2.0 \times 10^{-9}$  cm<sup>2</sup>/s, respectively, as reported in the papers.<sup>16,17</sup>

In the imide films of PMDA-B and BPDA-PDA, there were no detectable changes in curvature for an 8-h period. These two imide films do not uptake any NMP solvent at all. This result has been examined by a separate weight gain experiment. Except at temperatures much higher than room temperature, there is also no weight gain at all, even when immersing these films in NMP solvent for a few days.

### Case I Diffusion

In the imide film of 6FDA-PDA, the NMP diffusion is not case II. Instead, it is clearly a case I diffusion, as demonstrated in Figure 6. Its diffusion coefficient is  $0.85 \times 10^{-9}$  cm<sup>2</sup>/s. Such a "unique" behavior, i.e., case I other than case II, can be attributed to the presence of the unique 6FDA structure. Comparing with PMDA or BPDA, the 6FDA structure is very irregular and contains fluorine atoms that the others do not. As demonstrated in Figure 7, the film of 6FDA-PDA is relatively amorphous according to its X-ray diffraction pattern. Furthermore, its intermolecular spacing, 0.54 nm, is much larger than those of the other imide films.<sup>24-27</sup> This large spacing, coupling with the irregular chain structure, may enable the formation of large "voids" that, if large enough, would allow NMP molecules to move in and out more freely without causing polymeric chain relaxation and result in a case I diffusion.

### Diffusion in Polyimide Blends

By blending with 25% PMDA-B, the diffusion of NMP in the 6FDA-PDA film becomes "anomalous," i.e., its diffusion mechanism is neither case I nor II. This is shown in Figure 8. With more PMDA-B added into the 6FDA-PDA film, its diffusion mechanism exhibits case II, as shown in Figure 9. In the imide films of 50% PMDA-B with 50% 6FDA-PDA and 75% PMDA-B with 25% 6FDA-PDA, the diffusion front velocity constants are  $11.3 \times 10^{-8}$  cm/s and  $6.3 \times 10^{-8}$  cm/s, respectively. Comparing with

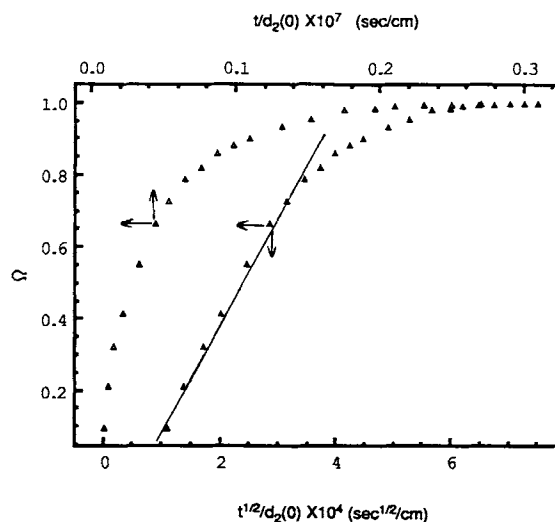


**Figure 6** The diffusion of NMP in the imide film of 6FDA-PDA. Unlike in all the other polyimides, it is a case I diffusion with  $D = 0.85 \times 10^{-9}$  cm<sup>2</sup>/s.

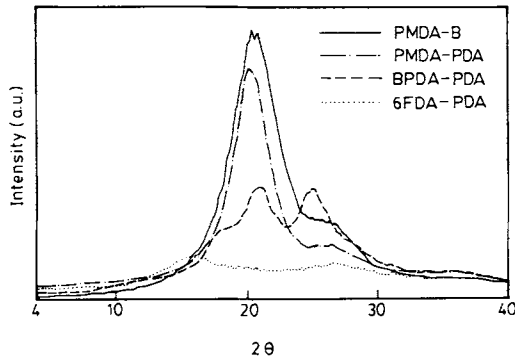


**Figure 7** Comparison between the out-of-plane X-ray diffraction pattern of the 6FDA imide film and those of the other polyimide films.

PMDA-ODA, the 6FDA-PDA molecule can more effectively enhance the diffusion of NMP in the PMDA-B imide films since both PMDA-ODA and 6FDA-PDA films have relatively amorphous structures and, when mixed with other crystalline polyimides, can destroy the crystalline structures of others. The difference between the degrees of their effects on enhancing the diffusions of NMP in their blends with PMDA-B should presumably be attributed to the difference of their chemical natures.

## CONCLUSION

In this study, a general formula correlating the bending curvature variation ratio of a layered struc-

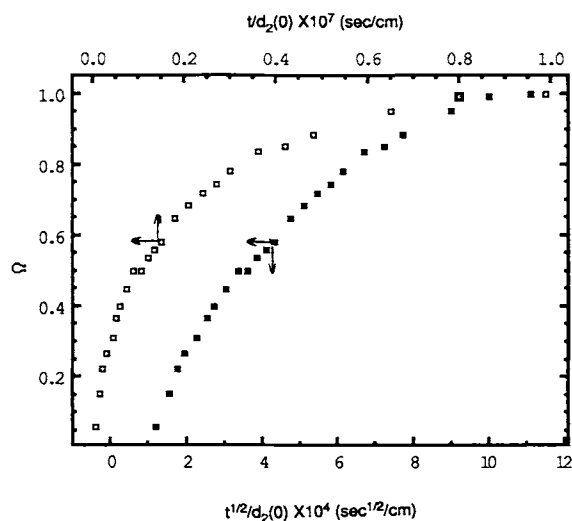


**Figure 8** The diffusion of NMP in the film of the blend with 25% PMDA-B and 75% 6FDA-PDA. Its diffusion mechanism is neither case I nor II.

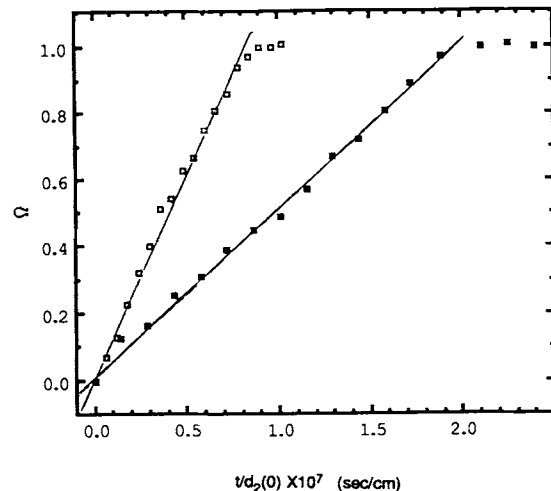


**Figure 9** The diffusions of NMP in the films of the blends with 50% PMDA-B and 50% 6FDA-PDA and 75% PMDA-B and 25% 6FDA-PDA. They both exhibit case II diffusion. ( $\square$ ), 50 wt % 6FDA-PDA/50 wt % PMDA-B,  $v = 1.13 \times 10^{-7}$  cm/s; ( $\blacksquare$ ), 25 wt % 6FDA-PDA/75 wt % PMDA-B,  $v = 0.63 \times 10^{-7}$  cm/s.

ture caused by solvent-induced swelling in its polymer overcoat with diffusion time under case II diffusion has been presented. In the event of case II diffusion, the diffusion front velocity can be calculated by using this formula. Coupling with a bending-beam apparatus, the diffusions of NMP solvent in the imide films of semiflexible and rigid rod-like polyimides and their blends have been investigated.

At room temperature, the diffusions of NMP solvent in the films of pure PMDA-PDA belonged to case II. While in pure PMDA-B and BPDA-PDA, no diffusion progress can be observed. By mixing PMDA-B with PMDA-ODA, the diffusions also exhibit case II behavior.

Unlike all the above polyimides, the diffusion of NMP in pure 6FDA-PDA belonged to case I, with a diffusion coefficient of  $0.85 \times 10^{-9}$  cm<sup>2</sup>/s. It becomes anomalous when mixing 6FDA-PDA with 25% PMDA-B. When mixing with 50 or 75% PMDA-B, it starts exhibiting case II diffusion.

The preabsorbed moisture in the film does not affect the NMP diffusion in the film of pure PMDA-PDA. The diffusion coefficient of water desorption in the film can also be measured simultaneously from the solvent diffusion experiment. It is  $0.52 \times 10^{-9}$  cm<sup>2</sup>/s as calculated.

The diffusion front velocity constant measured in the film of PMDA-PDA is  $7.3 \times 10^{-8}$  cm/s. In the blends of 6FDA-PDA with PMDA-B with compositions of 25/75 and 50/50, they are 6.3 and  $11.3 \times 10^{-8}$  cm/s, respectively. It seems that the addition

of 6FDA-PDA can very effectively enhance the diffusion of NMP in the PMDA-B imide films.

This work has been supported by the National Science Council, Taiwan, R.O.C., through projects NSC79-0405-E007-25 and NSC-80-0405-E007-13. The authors also acknowledge Hoechst Chemikalien for providing the 6F-dianhydride used in this study.

## REFERENCES

1. N. Adrova, N. I. Bessonov, I. A. Layus, and A. P. Rudakov, *Polyimide: A New Class of Thermostable Polymers*, Technomic, Newport, CT, 1970.
2. C. E. Sroog, *J. Polym. Sci., Macromol. Rev.*, **17**, 2583 (1976).
3. M. Terasav, S. Minami, and J. Rubin, *Int. J. Hybrid Microelectron.*, **6**, 607 (1983).
4. T. Watari and H. Murano, *IEEE Trans. Component Hybrid Manuf.*, **CHMT-8**, 462 (1985).
5. A. Saiki, K. Mukai, and S. Harada, *Polymer Material for Electronic Application*, ACS Symposium Series No. 184, 1982, p. 123.
6. Y. K. Lee and J. D. Craig, *Polymer Material for Electronic Application*, ACS Symposium Series No. 184, 1982, p. 107.
7. S. I. Numata, K. Fujisaki, N. Kinjo, J. Imaijumi, and Y. Mikami, Europ. Patent Application 84109054.1 (1984).
8. A. C. M. Yang, H. R. Brown, T. P. Russell, W. Volksen, and E. J. Kramer, *Polymer*, **29**, 1807 (1988).
9. E. Gattiglia and T. P. Russell, *J. Polym. Sci., Polym. Phys. Ed.*, **27**, 2131 (1989).
10. H. M. Tong and K. I. Saenger, *J. Polym. Sci., Polym. Phys. Ed.*, **27**, 689 (1989).
11. H. M. Tong and K. I. Saenger, *J. Plast. Film Sheeting*, **4**, 308 (1988).
12. R. M. Yang and H. M. Tong, *J. Polym. Sci., Polym. Lett. Ed.*, **23**, 583 (1985).
13. D. D. Denton, D. R. Day, D. F. Priore, S. D. Senturia, E. S. Anolick, and D. Scheider, *J. Electron. Mater.*, **14**, 119 (1985).
14. B. S. Berry and W. C. Pritchett, *IBM J. Res. Dev.*, **28**, 662 (1984).
15. R. C. Lasky, E. J. Kramer, and C. Y. Hui, *Polymer*, **29**, 673 (1988).
16. J. H. Jou, L. Hsu, P. T. Huang, W. P. Shen, and R. Huang, to appear.
17. J. H. Jou, R. Huang, P. T. Huang, and W. P. Shen, to appear.
18. A. H. Windle, in *Polymer Permeability*, J. Comyn, Ed., Elsevier, New York, 1985.
19. Z. C. Feng and H. D. Liu, *J. Appl. Phys.*, **54**, 83 (1983).
20. X. Gui, W. C. Wu, and G. B. Gao, *Acta Electron. Sinica*, **14**, 123 (1986).
21. J. H. Jou, *IBM-RJ (Physics)*, **6058** (1988).
22. J. M. Jou and J. H. Jou, *Proceedings of the 6th Annual Conference of the Chinese Society of Mechanical Engineering*, Tainan, Taiwan, R. O. C., 1989, p. 849.
23. C. E. Sroog, *J. Polym. Sci., Macromol. Rev.*, **11**, 161 (1976).
24. J. H. Jou and P. T. Huang, *Polymer J.*, **22**, 909 (1990).
25. R. M. Ikeda, *J. Polym. Sci., Polym. Lett. Ed.*, **4**, 353 (1966).
26. S. Isoda, H. Shimada, M. Kochi, and H. Kambe, *J. Polym. Sci., Polym. Phys. Ed.*, **19**, 1293 (1981).
27. J. H. Jou and P. T. Huang, to appear.

Received August 31, 1990

Accepted February 12, 1991